Applied Catalysis A: General 508 (2015) 10–15

Contents lists available at ScienceDirect

Applied Catalysis A: General

journal homepage: www.elsevier.com/locate/apcata

Highly efficient Mg(OH)Cl/SiO_2 catalysts for selective dehydrochlorination of 1,1,2-trichloroethane

Cen Tang [a], Yanxia Jin [a], Jiqing Lu [a], Xiaonian Li [b], Guanqun Xie [a,b,*], Mengfei Luo [a,*]

[a] Key Laboratory of the Ministry of Education for Advanced Catalysis Materials, Institute of Physical Chemistry, Zhejiang Normal University, Jinhua 321004, PR China

[b] Industrial Catalysis Institute, Zhejiang University of Technology, Hangzhou 310014, PR China

ARTICLE INFO

Article history:
Received 7 July 2015
Received in revised form
18 September 2015
Accepted 19 September 2015
Available online 25 September 2015

Keywords:
Dehydrochlorination
1,1,2-Trichloroethane
cis-1,2-Dichloroethene
Mg(OH)Cl
Heterogeneous catalysis

ABSTRACT

A series of Mg catalysts supported on SiO_2 were prepared by an incipient wetness impregnation method and tested for gas phase dehydrochlorination of 1,1,2-trichloroethane. It was found that these catalysts were very active and selective for the reaction. The catalytic performance depended on the Mg loading rather than the Mg precursors as the catalysts using $Mg(NO_3)_2{\cdot}6H_2O$ and $MgCl_2{\cdot}6H_2O$ as the precursors showed the similar performance. A catalyst containing 10 wt.% of Mg showed the best performance with a steady state TCE conversion of 92% and *cis*-dichloroethene selectivity of 91%. Moreover, characterizations of the catalysts revealed the formation of Cl-containing Mg species on the surface during the reaction. The analyses of the compositions of the stable catalysts under working conditions indicated a Cl/Mg ratio of 1, suggesting that Mg(OH)Cl could be the active sites for the reaction.

1. Introduction

Chlorinated hydrocarbons such as 1,1,2-trichloroethane (TCE) have been widespread in the environment by extensive application as degreasing agents [1]. However, the emission of these compounds is detrimental to the environment, which causes acid rain, ozone layer depletion and greenhouse effects [2–4]. Thus, the treatment of chlorinated hydrocarbons becomes a very important issue. One approach is the decomposition of these compounds, including direct incineration [5], catalytic combustion [6,7], biodegradation [8,9] and photo-catalytic decomposition [10,11]. Another approach is the conversion of these compounds to other valuable chemicals, including catalytic hydrodechlorination [12,13] and dehydrochlorination [14].

The dehydrochlorination of TCE leads to three main products: vinylidene chloride (VDC) [15], *cis*-1,2-dichloroethene (*cis*-DCE) [16–19] and *trans*-1,2-dichloroethene (*trans*-DCE) [14]. The main researches in the dehydrochlorination of TCE focus on the production of VDC from TCE [20–22]. For example, the catalytic dehydrochlorination of TCE into VDC was investigated over CsCl catalysts supported on silica gels using a pulse technique [23], with a conversion of 90% and a selectivity of 90% in the first pulse at 250 °C. Moreover, the hydroxyl groups on the silica surface were assumed to accelerate the elimination of hydrogen chloride.

However, there are few reports on the direct dehydrochlorination of TCE to *cis*-DCE. The wide applications of *cis*-DCE include fungicides, anesthetics and frozen agents. *Cis*-DCE also could be used as solvents for paint, resin, wax, rubber and acetate fibers. The production of *cis*-DCE could be achieved through reductive dechlorination of tetrachloroethene by a thermophilic anaerobic enrichment culture [24], the photo initiated chlorination of C_2H_2 in N_2 [25], and aqueous-phase reductive dechlorination (hydrogenolysis) of trichlorothylene [26]. Unfortunately, the resulting products in these processes generally contain a mixture of both *cis*-DCE and *trans*-DCE [25–28] and the selectivity to *cis*-DCE is quite low [26].

Therefore, highly efficient catalyst system for the synthesis of *cis*-DCE is desirable. MgO supported on SiO_2 are typically used as Ziegler–Natta catalysts [29–31], which are the best candidates for the low pressure production of linear low-density polyethylene and ethylene co-polymers from the gas phase. In the current work, Mg(OH)Cl/SiO_2 catalysts were used for dehydrochlorination of TCE. It is interesting that these catalysts are very active and selective for the production of *cis*-DCE. Moreover, the possible active sites of the catalysts have been investigated.

* Corresponding authors. Fax: +86 579 82282595.
E-mail addresses: gqxie@zjnu.edu.cn (G. Xie), mengfeiluo@zjnu.cn (M. Luo).

http://dx.doi.org/10.1016/j.apcata.2015.09.024
0926-860X/

2. Experimental

2.1. Catalyst preparation

A series of Mg(N)/SiO_2 catalysts with different Mg loadings were prepared using an incipient wetness method. In a typical preparation, the SiO_2 support (S_{BET} = 378.8 $m^2\ g^{-1}$) was added to an appropriate amount of aqueous solution of $Mg(NO_3)_2{\cdot}6H_2O$ (Aladdin, 99 %), and the mixture was sonicated for 30 min at room temperature by a commercial ultrasonic cleaner (Branson, 1510R-MT, 70 W, 42 kHz). Then the mixture was kept for 6 h at room temperature. Finally, it was mildly evaporated at 90 °C to completely remove water, and then dried at 120 °C overnight. The resulting solid was pretreated under a N_2 flow (30 ml min^{-1}) at different temperatures (300–500 °C) for 1.5 h. The obtained catalysts were designated as *x*Mg(N)/SiO_2−*y*, with *x* and *y* refer to the weight percent of Mg and pretreatment temperature, respectively. A reference catalyst 10Mg(Cl)/SiO_2−300 with a precursor of $MgCl_2{\cdot}6H_2O$ was also prepared in a similar manner.

2.2. Catalyst characterization

Actual contents of Mg and Cl in the catalysts were determined by X-ray fluorescence (XRF) analysis, on a Shimadzu XRF-1800 spectrometer. The Qual-Quantitative analysis automatically executed a quantitative analysis in the FP method after the qualitative analysis of a sample of unknown composition. The X-ray generator was operated at 40 kV and 70 mA, while the step angle and speed were 0.1° and 8° min^{-1}, respectively.

The BET surface areas of the catalysts were measured by N_2 adsorption at liquid-nitrogen temperature (77 K), using a surface area analyzer (Quantachrome Autosorb-1). The catalysts were pretreated at 120 °C for 6 h in vacuum.

X-ray diffraction (XRD) patterns were recorded with a PANalytical X′Pert PRO MPD powder diffractometer using Cu Kα radiation. The working voltage was 40 kV and the working current was 40 mA. The patterns were collected in a 2θ range from 10 to 80°, with a scanning speed of 0.15° s^{-1}.

High-resolution transmission electron microscopy (HRTEM) was performed on a JEM-2100F microscopy with a field emissive gun, operated at 200 kV and with a point resolution of 0.24 nm.

Thermogravimetric analysis (TG-DTA) was conducted on a NETZSCH STA 449C thermal graphic analyzer. N_2 was used as the carrier gas (30 ml min^{-1}, atmospheric). The heating rate was 10 °C min^{-1}.

Fourier transform infrared (FTIR) spectra of the samples were recorded on a NEXUS670 spectrometer equipped with a MCT detector in the range of 400–4000 cm^{-1} using KBr pellets. All obtained spectra were auto-baseline corrected.

2.3. Activity test

Catalytic dehydrochlorination of TCE was carried out in a conventional fixed-bed reactor (i.d. = 8 mm). 0.3 g of the catalyst was diluted into a volume of 0.6 ml with a small amount of quartz sand and loaded in the reactor. A thermalcouple was placed in the middle of the catalyst bed to monitor the actual reaction temperature. Before reaction, the catalyst was heated from room temperature to desired temperature (300 - 500 °C) at a heating rate of 5 °C min^{-1} in N_2 (30 ml min^{-1}) and kept for 90 min at the desired temperature, and then was cooled to the reaction temperature of 300 °C. The reactant flow was generated by flowing N_2 through a bubbler containing liquid TCE (TCE content = 4.6 vol.%, N_2 flow rate = 30 ml min^{-1}, GHSV = 1000 h^{-1}). The reactant flow was introduced to the catalyst bed consisting of the Mg catalysts. The concentrations of TCE and other organic products during the reaction were analyzed by an Agilent 6850 gas chromatograph equipped with a FID detector. The carbon balance was calculated to be ±5%.

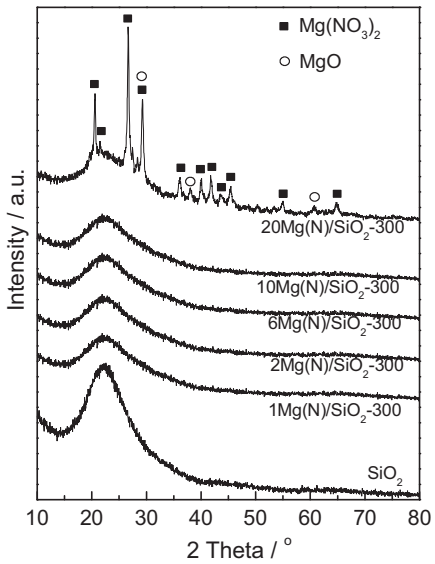

Fig. 1. XRD patterns of Mg(N)/SiO_2 catalysts with different Mg loadings.

3. Results and discussion

Table 1 summarizes the physical properties of the Mg catalysts. It is found that the actual content of Mg is very close to the corresponding nominal value, suggesting that there is no loss of Mg in the preparation process. The surface area of the Mg catalyst gradually declines with Mg loading. The 20Mg(N)/SiO_2−300 catalyst has the lowest surface area (32.7 $m^{-2}\ g^{-1}$), probably due to the blockage of internal pores of SiO_2 by the Mg species. Fig. 1 presents the XRD patterns of the Mg catalysts with different Mg loadings. Only one broad diffraction peak centered at about 2θ of 22.3° could be observed for the catalyst with Mg content lower than 10 wt.%, which is attributed to the amorphous SiO_2 support. No diffraction of Mg species could be detected, probably due to the high dispersion of these species on the surface. When the Mg loading is 20 wt.%, the diffraction peaks due to MgO (PDF 30-0794) and $Mg(NO_3)_2$ (PDF 19-0765) emerge. The formation of MgO is a result of the thermal decomposition of $Mg(NO_3)_2$ ($2\ Mg(NO_3)_2 \rightarrow 2\ MgO + 4\ NO_2 + O_2$). Thus, it could be concluded that the fresh catalyst (N_2-pretreated) contains MgO and $Mg(NO_3)_2$. This conclusion is supported by TG-DTA curves of the un-pretreated 10Mg(N)/SiO_2 catalyst (Fig. 2). The first major weight loss of the sample ranges from 99 to 330 °C, and the DTA curve gives two characteristic peaks at 133 and 264 °C, which are due to the gradual removal of crystal water in $Mg(NO_3)_2{\cdot}6H_2O$ molecule [32]. Besides, the thermal decomposition of $Mg(NO_3)_2$ starts from 330 °C and completes at 483 °C to form MgO. The weight loss at these stages is about 55.4% of the total weight, which is consistent with the theoretical value (54.5%,$2\ Mg(NO_3)_2{\cdot}6H_2O \rightarrow 2\ MgO + 4\ NO_2 + O_2 + 12H_2O$). It is worth noting that the thermal decomposition of $Mg(NO_3)_2{\cdot}6H_2O$ is not completed at low calcination temperatures (i.e. 300 °C), as the XRD results reveal the presence of both MgO and $Mg(NO_3)_2$, particularly at high Mg loadings (e.g. 20Mg(N)/SiO_2). The influence of Mg loadings on the catalytic performance is shown in Fig. 3. It can be seen that the conversion of TCE first increases and then decreases with the Mg loading, and the highest conversion (92%) is obtained on the 10Mg(N)/SiO_2−300 catalyst. Also, it seems that there is an induction period for the TCE conversion, which gradually increases in the first 2 h reaction and gradually reaches a steady

Table 1
Physical properties of the Mg catalysts.

Catalyst	Mgloading/% Mg/(Mg + SiO_2)		Surface area/$m^2\ g^{-1}$	Cl/Mg molar ratio[a]
	Nominal	Actual		
1Mg(N)/SiO_2-300	1.1	1.0	295.6	n.d.
2Mg(N)/SiO_2-300	2.3	2.4	263.9	0.9
6Mg(N)/SiO_2-300	6.0	6.0	238.0	0.9
10Mg(N)/SiO_2-300	10.0	10.1	175.3	1.1
20Mg(N)/SiO_2-300	20.0	19.4	32.7	n.d.
10Mg(Cl)/SiO_2-300	10.0	10.2	176.3	0.9

n.d.: not detected
[a] : measured on the spent sample after 4 h reaction.

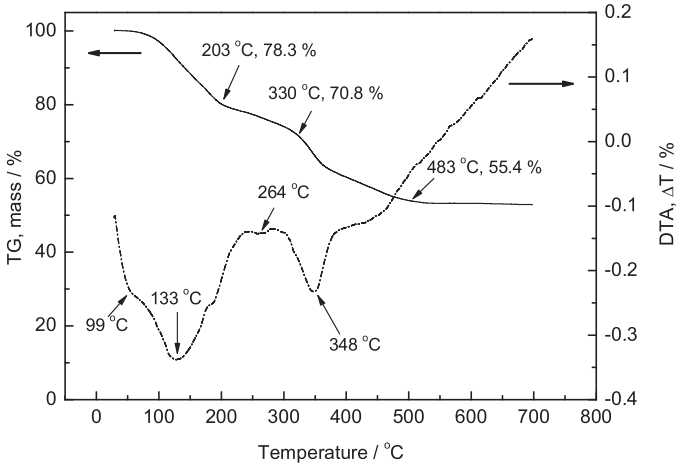

Fig. 2. TG–DTA curves of non-pretreated 10 Mg(N)/SiO_2 catalyst.

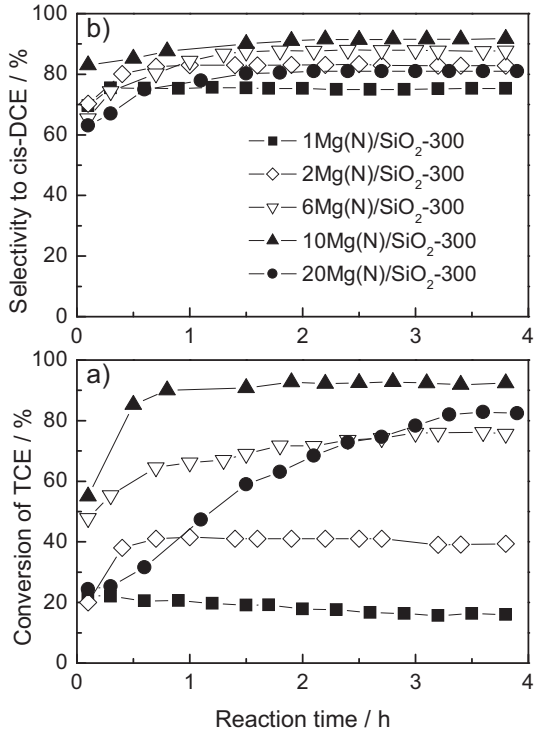

Fig. 3. Effect of Mg loadings on the dehydrochlorination of TCE over Mg(N)/SiO_2-300 catalysts. Reaction temperature = 300 °C.

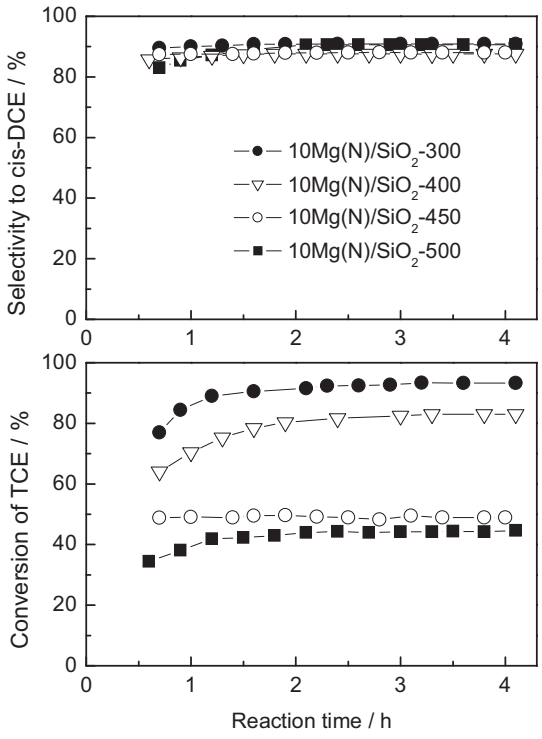

Fig. 4. Effect of pretreatment temperature on the dehydrochlorination of TCE over 10Mg(N)/SiO_2 catalysts. Reaction temperature = 300 °C.

state. Fig. 3b illustrates the selectivity of *cis*-DCE with different Mg contents. In addition to the main product of *cis*-DCE, some by-products such as VDC and *trans*-DCE are also detected. It is found that the selectivity of *cis*-DCE first increases then decreases with increasing Mg content, with the highest selectivity (91%) obtained on the 10Mg(N)/SiO_2−300 catalyst. As the Mg contents in the catalysts are different, a comparison of specific reaction rates based on Mg loading may reflect more relevant information of the reactivity. The specific reaction rates are 2.6×10^{-5}, 3.1×10^{-5}, 2.3×10^{-5}, 1.7×10^{-5} and 7.2×10^{-6} $mol_{TCE}\ g_{Mg}\ s^{-1}$ for the 1Mg(N)/SiO_2-300, 2Mg(N)/SiO_2-300, 6Mg(N)/SiO_2-300, 10Mg(N)/SiO_2-300 and 20Mg(N)/SiO_2-300 catalysts, respectively. It is noticed that the calculated specific rates are close for the catalysts with Mg loadings less than 10 wt.%, while for the 20Mg(N)/SiO_2-300 catalyst the rate is much lower. This is an implication that the Mg species may highly dispersed at low Mg contents (e.g. less than 10 wt.%) but they might aggregate at high Mg content (e.g. 20 wt.%) and the lesser activity of 20 Mg(N)/SiO_2-300 catalyst should also be due to the presence of $Mg(NO_3)_2$ particles, which are consistent with the XRD results (Fig. 1).

Fig. 4 demonstrates the effect of pretreatment temperature on the performance of the Mg catalysts. It is

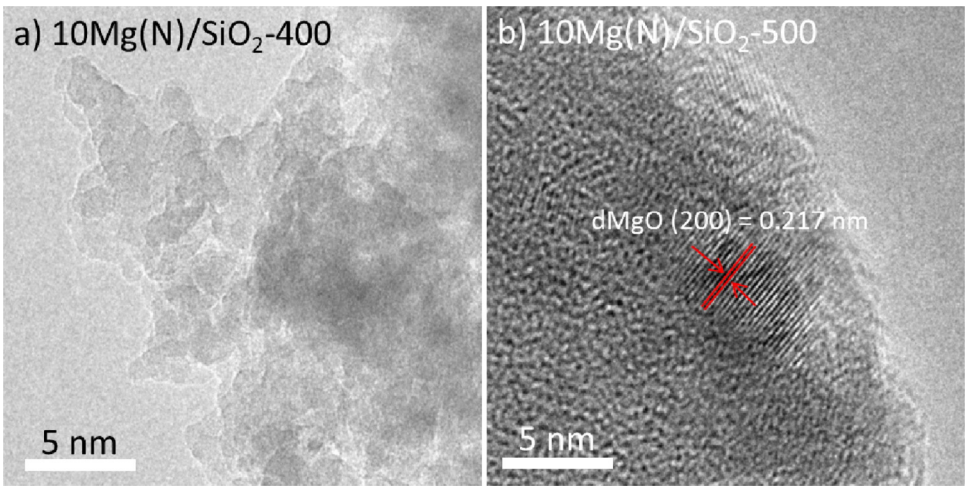

Fig. 5. TEM images of 10Mg(N)/SiO_2 catalysts pretreated at different temperatures: (a) 400 °C (10Mg(N)/SiO_2-400); (b) 500 °C (10Mg(N)/SiO_2-500).

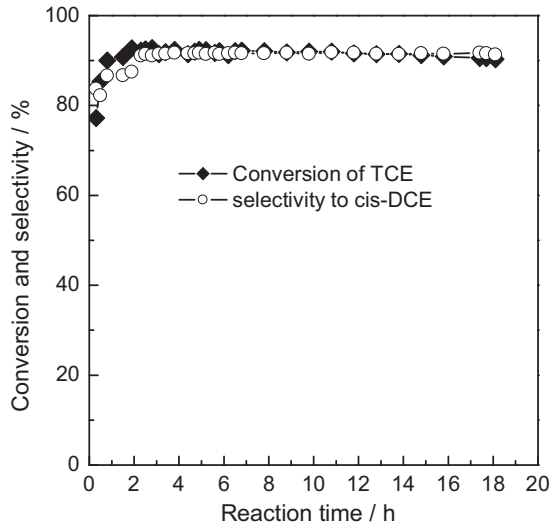

Fig. 6. Stability of 10Mg(N)/SiO_2-300 catalyst for the dehydrochlorination of TCE. Reaction temperature = 300 °C.

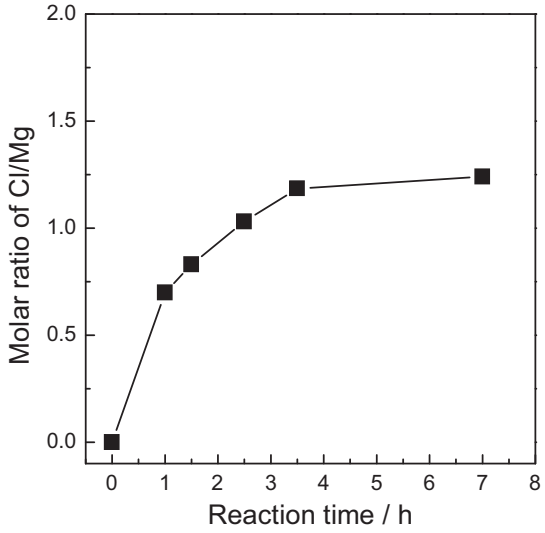

Fig. 7. Molar ratio of Cl/Mg of 10Mg(N)/SiO_2-300 catalyst during the dehydrochlorination reaction. Reaction temperature = 300 °C.

revealed that the overall activities follow the order of 10Mg(N)/SiO_2−300 > 10 Mg(N)/SiO_2−400>10 Mg(N)/SiO_2−450 > 10 Mg(N)/SiO_2-500, which implies that high pretreatment temperature is detrimental to the activity of the Mg catalysts. While the selectivity to *cis*-DCE (about 85–90%) merely changes upon the pretreatment temperature. Fig. 5 shows the TEM images of the Mg samples. The 10Mg(N)/SiO_2-400 catalyst shows no obvious MgO particles (Fig. 5a), while the 10 Mg(N)/SiO_2-500 sample (Fig. 5b) shows distinct MgO entity by measuring the D-space distance of the particle. Therefore, the decline of the activity on the high-temperature pretreated sample (e.g. 10Mg(N)/SiO_2-500) is probably due to the aggregation of MgO particles during the thermal treatment.

Furthermore, the stability of the Mg catalysts was also tested, as shown in Fig. 6. The 10Mg(N)/SiO_2-300 catalyst is quite stable during 18 h reaction, without obvious loss of activity during the reaction process. Also, the Mg content in the spent catalyst is 9.5 wt.%, which indicates that there is no loss of Mg species during the reaction.

The catalysts in the current work show superior performance to those reported in literature. For example, Zhu and Yarwood [25] reported photo initiated chlorination of C_2H_2 in N_2, in which the resulting products contain both main products of *cis*-DCE and *trans*-DCE. Also, De Journett et al. [26] reported aqueous-phase reductive dechlorination of trichloroethylene using a complicated Ti(III) citrate mediated by 5,10,15,20-tetrakis-(4-carboxyphenyl) porphyrin cobalt (II), in which the yield of *cis*-DCE was about 53%. Therefore, the catalyst system employed in the current work has several advantages such as simple preparation, high yield of *cis*-DCE (83.7%).

It is worthwhile to explore the nature of the active sites on the catalysts. Considering that HCl could be produced during the reaction which would further react with Mg compounds to form Cl-containing species such as $MgCl_2$, it is possible that these Cl-containing Mg species play an important role in the reaction. Therefore, the contents of Cl in the different reaction stages were measured by XRF, as shown in Fig. 7. The detection of the Cl contents in different reaction stages were conducted by stopping the reaction at desired reaction time and taking the catalyst out from the reactor for the measurement. It is clear that the Cl content in the catalyst gradually increases with reaction time. The Cl/Mg molar ratio reaches a steady value (about 1.1) after 4 h reaction. This change is consistent with the observed catalytic performance (Fig. 3), in which an induction period was found in the first 3 h reaction for

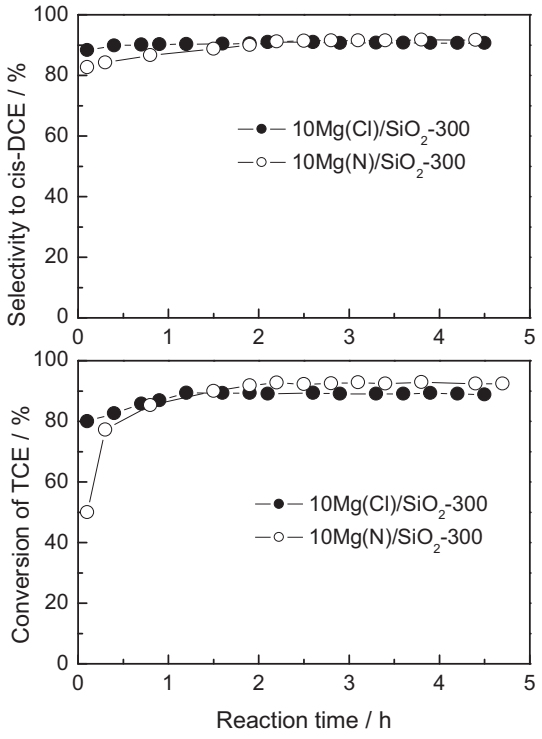

Fig. 8. Effect of different precursors on the dehydrochlorination of TCE over 10Mg/SiO_2-300 catalysts. Reaction temperature = 300 °C.

the 10Mg(N)/SiO_2-300 catalyst. This observation is a strong indication that the formed Cl-containing Mg species might be the active sites of the reaction. Moreover, judging from the ratio of Cl and Mg (about 1.1) in the spent catalyst, the possible formula of the Mg-Cl species is Mg(OH)Cl.

In addition, element analyses of spent catalysts with different loadings also indicate that the Cl/Mg ratios are close to 1 (Table 1) after steady state (about 4 h reaction), further implying the formation of Mg(OH)Cl.

According to the XRD and TG-DTA results (Figs. 1 and 2), the fresh catalyst pretreated at low temperature contains both MgO and $Mg(NO_3)_2$. Such Mg species could react with HCl in situ produced during the dehydrochlorination of TCE, and would further form Cl-containing specie as Mg(OH)Cl according to the XRF results (Fig. 7). The possible path of the Mg(OH)Cl formation would be as follows:

$$MgO + HCl \rightarrow Mg(OH)Cl. \quad (1)$$

$$Mg(NO_3)_2{\cdot}H_2O + HCl \rightarrow Mg(OH)Cl + 2HNO_3. \quad (2)$$

To further investigate the nature of the active sites in the 10 Mg(N)/SiO_2-300 catalyst, a reference catalyst (10Mg(Cl)/SiO_2-300) using $MgCl_2{\cdot}6H_2O$ as the precursor was also tested for this reaction and the results are shown in Fig. 8. It is found that the catalysts prepared using $Mg(NO_3)_2{\cdot}6H_2O$ and $MgCl_2{\cdot}6H_2O$ as the precursors almost show identical behaviors, except that the 10Mg(N)/SiO_2-300 catalyst shows an induction period while the 10Mg(Cl)/SiO_2-300 catalyst quickly reaches a steady state. These results imply that the active sites in the two types of Mg catalysts are the same regardless of the Mg precursors.

To investigate the active sites on 10Mg(Cl)/SiO_2-300 catalyst, thermal decomposition of the pure $MgCl_2{\cdot}6H_2O$ was conducted, as shown in Fig. 9. The decomposition of the $MgCl_2{\cdot}6H_2O$ involves five stages as follows [33,34]:

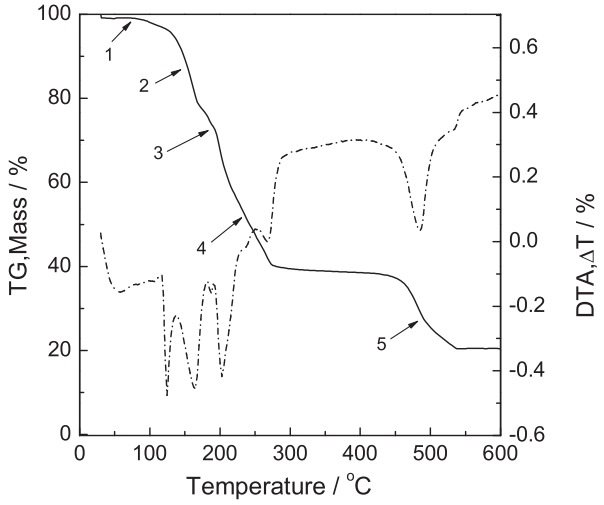

Fig. 9. TG-DTA curves of pure $MgCl_2.6H_2O$.

Stage 1: from 25 to 115 °C

$$xMgCl_2{\cdot}6H_2O + yMgCl_2{\cdot}4H_2O \rightarrow (x + y)MgCl_2{\cdot}4H_2O + 2xH_2O$$

$$(x + y) = 1$$

Stage 2: from 115 to 160 °C

$$MgCl_2{\cdot}4H_2O \rightarrow MgCl_2{\cdot}2H_2O + 2H_2O$$

Stage 3: from 160 to 190 °C

$$MgCl_2{\cdot}2H_2O \rightarrow MgCl_2{\cdot}H_2O + H_2O$$

Stage 4: from 190 to 235 °C

$$MgCl_2{\cdot}H_2O \rightarrow aMgCl_2{\cdot}nH_2O + bMg(OH)Cl + bHCl + (1–an–b)H_2O$$

$$4 < n < 1; a + b = 1$$

Stage 5: from 235 to 415 °C

$$Mg(OH)Cl \rightarrow MgO + HCl$$

This above analysis suggests that the formation of Mg(OH)Cl through the decomposition of $MgCl_2{\cdot}6H_2O$ could occur at the temperature below 300 °C (stage 4). As the Mg catalyst (10Mg(Cl)/SiO_2-300) using $MgCl_2{\cdot}6H_2O$ as the precursor was pretreated and reacted at 300 °C in the dehydrochlorination of TCE, it could be concluded that Mg(OH)Cl forms in this catalyst. In addition, the presence of such Mg(OH)Cl species is also evidenced by the element analysis of the spent 10Mg(Cl)/SiO_2-300 (Table 1), which shows a Cl/Mg ratio of 0.93. Therefore, it could be concluded that the active sites in the 10Mg(Cl)/SiO_2-300 catalyst for the dehydrochlorination of TCE are Mg(OH)Cl.

As the catalysts prepared using $Mg(NO_3)_2{\cdot}6H_2O$ and $MgCl_2{\cdot}6H_2O$ as the precursors almost show identical behaviors (Fig. 8), the active sites in 10Mg(N)/SiO_2-300 catalyst and 10Mg(Cl)/SiO_2-300 catalyst should be the same (e.g. Mg(OH)Cl), which is formed through the reaction with HCl in situ produced during the dehydrochlorination of TCE.

The surface features of the catalysts were investigated by infrared spectroscopy, as shown in Fig. 10. For all the catalysts, a broad band at 3420 cm^{-1}, a sharp band at 1633 cm^{-1} and a broad band at 1094 cm^{-1} are observed, which could be assigned to the stretching vibration, bending vibration of the hydroxyl group and asymmetric vibration of Si—O—Si in the SiO_2 support, respectively [35]. For the fresh 10Mg(N)/SiO_2-300 catalyst, a sharp band at 1378 cm^{-1} is observed, which is characteristic of MgO oxide [36].

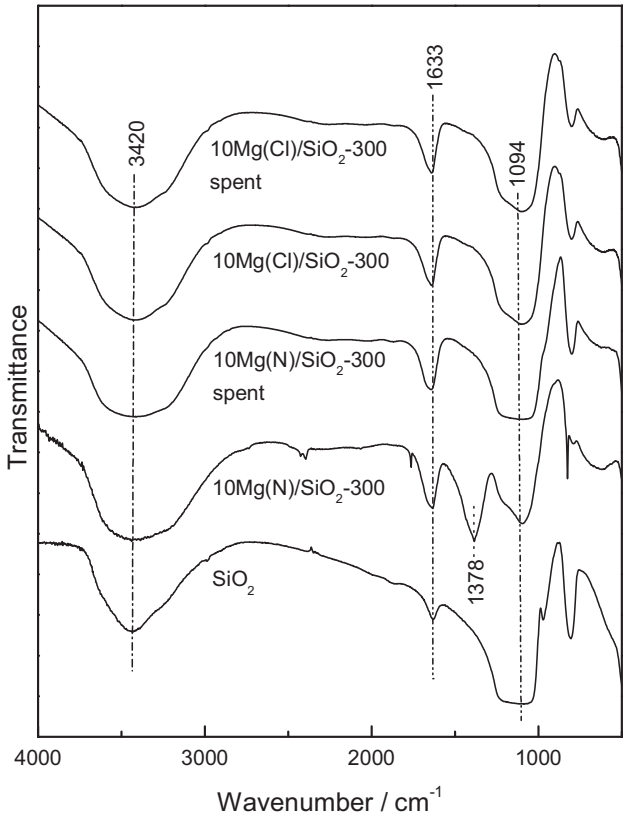

Fig.10. FTIR spectra of various catalysts.

The assignment of this band was confirmed by the observation of the same band on a supported MgO/SiO_2 sample, suggesting the presence of MgO in the $10Mg(N)/SiO_2$-300 catalyst. After reaction, the spectrum of the spent $10Mg(N)/SiO_2$-300 catalyst do not change much compared to the fresh one, except for the disappearance of the band at 1378 cm^{-1}, implying the transformation of MgO species during the reaction. Interestingly, the features of the spent $10Mg(N)/SiO_2$-300 are almost identical to those of the fresh and spent $10Mg(Cl)/SiO_2$-300 catalysts, suggesting the same surface species on these catalysts. Unfortunately, the direct detection of the surface Mg(OH)Cl compound could not be reached because the main band of Mg(OH)Cl located at 3500 cm^{-1} [37] is likely overlapped by the hydroxyl group of SiO_2 in this region. Nevertheless, since the presence of Mg(OH)Cl on the $10Mg(Cl)/SiO_2$-300 is readily evidenced (Fig. 9), the same spectra of the spent $10Mg(N)/SiO_2$-300 and $10Mg(Cl)/SiO_2$-300 (either fresh and spent) lead to a reasonable conclusion that Mg(OH)Cl species are also present on the spent $10Mg(N)/SiO_2$-300.

4. Conclusions

In this work, gas phase dehydrochlorination of TCE to *cis*-DCE was performed on Mg species supported on SiO_2 using $Mg(NO_3)_2{\cdot}6H_2O$ as the precursor. It was found that these Mg catalysts had excellent performance, with a TCE of conversion (92%) and a *cis*-DCE selectivity of 91% obtained on the $10Mg(N)/SiO_2$-300 catalyst. This catalyst had the similar performance as the catalyst prepared using $MgCl_2{\cdot}6H_2O$ as the precursor, suggesting that these two catalysts had same active sites. Further analyses of the element compositions of the spent catalysts revealed the formation of Cl-containing Mg species with a Cl/Mg molar ratio of about 1, implying that Mg(OH)Cl could be the active sites for the reaction.

Acknowledgments

This work is financially supported by National Natural Science Foundation of China (Grant No. 21476207), and the open research fund of top key discipline of chemistry in Zhejiang provincial colleges (Zhejiang Normal University Grant No. ZJHX201413).

References

[1] R. Bartsch, C.L. Curlin, T.F. Florkiewicz, H.R. Minz, T. Navin, R. Scannell, E. Zelfel, Chlorine: Principles and Industrial Practice, Weinheim, 2000.
[2] US Environmental Protection Agency (EPA), The clean air act of 1990, a primer on consensus building, Government Printing Office Press, Washington, 1990.
[3] Intergovernmental Panel on Climate Change, The IPCC scientific assessment. Cambridge University Press, Cambridge, 1990.
[4] Ozone Secretariat United Nations Environment Programme, Handbook for the montreal protocol on substances that deplete the ozone layer 7th ed. Secretariat of the Vienna convention for the protection of the ozone layer and the Montreal protocol on substances that deplete the ozone layer, Nairobi, 2006.
[5] J. Stach, V. Pekáarek, R. Endršt, J. Hetflejš, Chemosphere. 39 (1999) 2391–2392.
[6] N. Coute, J.D. Ortego Jr., J.T. Richardson, M.V. Twigg, Appl. Catal. B. 19 (1998) 175–187.
[7] B. de Rivas, C. Sampedro, R. López-Fonseca, M.Á. Gutiérrez-Ortiz, J.I. Gutiérrez-Ortiz, Appl. Catal. A: Gen. 417–418 (2012) 93–101.
[8] D. Barriault, M. Sylvestre, Can. J. Microbiol. 39 (1993) 594–602.
[9] J. Yu, W. Cai, S. Zhao, Y. Wang, J. Chen, Chin. J. Chem. Eng. 21 (2013) 781–786.
[10] M. Trillas, J. Peral, X. Domènech, J. Chem. Tech. Biotol. 67 (1996) 237–242.
[11] S. Ahmed, D.F. Ollis, Sol. Energy 32 (1984) 597–601.
[12] Y. Park, T. Kang, Y.S. Cho, P. Kim, J.C. Park, J. Yi, Stud. Surf. Sci. Catal. 146 (2003) 637–640.
[13] A. Gampine, D.P. Eyman, J. Catal. 179 (1998) 315–325.
[14] A.W.A.M. van der Heijden, A.J.M. Mens, R. Bogerd, B.M. Weckhuysen, Catal. Lett. 122 (2008) 238–246.
[15] R.W. Kapp, Vinyl Chloride, Reference Module in Biomedical Sciences, 2014, pp. 934–938.
[16] J. Dolfing, D. Janssen, Biodegradation 5 (1994) 21–28.
[17] K. Kokubo, K. Kitasaka, T. Oshima, Org. Lett. 8 (2006) 1597–1600.
[18] D.A. Turton, D.F. Martin, K. Wynne, Phys. Chem. Chem. Phys. 12 (2010) 4191–4200.
[19] N.C. Craig, L.G. Piper, V.L. Wheeler, J. Phys. Chem. 75 (1971) 1453–1460.
[20] I. Mochida, H. Watanabe, A. Uchino, H. Fujitsu, K. Takeshita, M. Furuno, T. Sakura, H. Nakajima, J. Mol. Catal. 12 (1981) 359–364.
[21] J. Garnier, P.-E. Dufils, J. Vinas, Y. Vanderveken, A. van Herk, P. Lacroix-Desmazes, Polym. Degrad. Stab. 97 (2012) 170–177.
[22] M. Trushechkina, B. Azbel, Principles and Methods for Accelerated, Catalyst Design and Testing, Springer, Portugal, 2001, pp. 399–405.
[23] I. Mochida, T. Takagi, H. Fujitsu, Appl. Catal. 18 (1985) 105–115.
[24] S.W.M. Kengen, C.G. Breidenbach, A. Felske, A.J.M. Stams, G. Schraa, W.M. de Vos, Appl. Environ. Microb. 65 (1999) 2312–2316.
[25] T. Zhu, G. Yarwood, J. Chen, H. Niki, J. Phys. Chem. 98 (1994) 5065–5067.
[26] T.D. DeJournett, J.M. Fritsch, K. McNeill, W.A. Arnold, J. Labelled Comp. Radiophram. 48 (2005) 353–357.
[27] P.M. Bradley, F.H. Chapelle, Environ. Sci. Technol. 31 (1997) 2692–2696.
[28] P.M. Bradley, F.H. Chapelle, Environ. Sci. Technol. 32 (1998) 553–557.
[29] J.C. Chadwick, Encyclopedia Polym. Sci. Technol. 6 (2003) 517–536.
[30] V. Corradini, Compr. Polym. Sci., Pergamon (1988) 29.
[31] F. Auriemma, C. De Rosa, J. Appl. Cryst. 41 (2008) 68–82.
[32] J. Madarász, P.P. Varga, G. Pokol, J. Anal. Appl. Pyrolysis 79 (2007) 475–478.
[33] G.T. Whiting, D. Grondin, D. Stosic, S. Bennici, A. Auroux, Solar Energy Mater. Solar Cells 128 (2014) 289–295.
[34] Q. Huang, G. Lu, J. Wang, J. Yu, J. Anal. Appl. Pyrol. 91 (2011) 159–164.
[35] Y.Y. Pei, M. Wang, D. Tian, X.F. Xu, L.J. Yuan, J. Colloid Interface Sci. 453 (2015) 194–201.
[36] I.F. Mironyuk, V.M. Gun'ko, M.O. Povazhnyak, V.I. Zarko, V.M. Chelyadin, R. Leboda, J. Skubiszewska-Zięba, W. Janusz, Appl. Surf. Sci. 252 (2006) 4071–4082.
[37] S. Kashani-Nejad, K.W. Ng, R. Harris, Characterization of MgOHCl/MgO mixtures with infrared spectroscopy, Magnesium Technology, TMS, 2004 pp. 161–165.